J Mater Sci: Mater Electron
DOI 10.1007/s10854-015-2869-7

Cadmium sulfide interface layer for improving the performance of titanium dioxide/poly (3-hexylthiophene) solar cells by extending the spectral response

M. Thanihaichelvan · K. Sockiah · K. Balashangar · P. Ravirajan

Received: 18 December 2014 / Accepted: 23 February 2015

Abstract This work focused on studying the effect of cadmium sulfide (CdS) interfacial layer on the performance of titanium dioxide (TiO_2)/poly (3-hexylthiophene) (P3HT) solar cells and finding out its effect on charge recombination dynamics of hybrid TiO_2/P3HT solar cells. FESEM images confirm the uniform distribution of chemical bath deposited CdS layer on TiO_2 nanoparticles. Insertion of CdS layer at the nanocrystalline TiO_2/P3HT interface broadens quantum efficiency spectrum of the solar cells with peak values over 80 and 40 % at the wavelengths of maximum absorption of CdS and P3HT respectively and hence enhances short-circuit current density (J_{SC}) from 3.5 to 5.9 $mAcm^{-2}$ under simulated illumination (70 $mWcm^{-2}$) with an AM 1.5 filter. CdS layer further improves open circuit voltage (V_{OC}) from 0.35 to 0.57 V, which is consistent with higher built-in voltage in CdS/P3HT than in TiO_2/P3HT due to relatively lower laying conduction band edge of CdS. Photovoltaic transient measurements show that the carrier life-time in TiO_2/CdS/P3HT solar cell is an order of magnitude longer than that in TiO_2/P3HT solar cell. Optimized TiO_2/P3HT solar cells with CdS interlayer yield power conversion efficiencies over 1.5 %, which is three times greater than that for similar solar cells without CdS layer.

M. Thanihaichelvan · K. Sockiah · K. Balashangar · P. Ravirajan (✉)
Department of Physics, Faculty of Science, University of Jaffna, Jaffna 40000, Sri Lanka
e-mail: pravirajan@gmail.com

M. Thanihaichelvan
e-mail: thanihai@jfn.ac.lk

K. Sockiah
e-mail: karshi86@gmail.com

K. Balashangar
e-mail: k_balashangar@yahoo.com

1 Introduction

Main text paragraph Hybrid metal oxide/polymer solar cells are currently under intensive focused due to their relative ease of fabrication by cost-efficient methods and materials. The use of stable metal oxides such as ZnO [1], SnO_2 [2], and TiO_2 [3] as the electron acceptor in multi-layered photovoltaic (PV) devices has been widely studied since they offer good electron transport properties, fabrication via simple techniques, nontoxicity, and heterojunction morphology control. However, the power conversion efficiencies (PCEs) of metal oxide–polymer solar cells are limited by poor matching of polymer's absorbance with the solar spectrum, increased recombination of carriers in the irregular donor–acceptor interfaces during the transport, and low open circuit voltages. The active layer thickness to absorb the light in the cell structure is also limited by exciton diffusion lengths and mobility of polymers. Several recent studies are focused on eliminating these issues to fabricate highly efficient hybrid solar cells. It has been reported that use of oriented nanostructures [1, 4], weakly absorbing interface modifiers [5, 6], multilayers [3, 7, 8] and tandem structures [9, 10] helped to improve the PCEs of hybrid PV devices.

Interface modifiers are widely used in the donor–acceptor interface to improve the V_{OC} and fill factor by suppressing surface recombination. Weakly absorbing interface modifiers such as Al_2O_3 were also used to improve the J_{SC} by controlling the recombination kinetics [11]. Multiple sensitizers were used to improve the spectral response. It uses multiple photon absorbing materials as sensitizers in a cascaded device structure. Many inorganic materials especially metal sulfides including PbS, CdS, SbS and ZnS were used as co-sensitizers with polymer photon absorbers. Studies have also done on multiple inorganic

Published online: 28 February 2015

materials which complementing the absorption of each other. PbS–CdS [12, 13], CdS–CdSe [14], CdSe–ZnS binaries, and PbS–CdS–ZnS [15] and CdS–CdSe–ZnS [16] ternary systems as co-sensitizers were reported with considerable PCEs but using liquid electrolytes.

CdS is a II–IV material which is widely known as the window layer for the popular cadmium telluride thin film solar cells with a wide band gap of 2.42 eV, which facilitates strong absorption in the UV region and transparent in the infrared region. Due to its moderate optical band gap, it can also be used as a sensitizer. The use of CdS as the sensitizer is particularly promising, since it can be fabricated as zero-dimensional quantum dots with diameters $<$10 nm. Promising PCEs were reported for solar cells made with CdS sensitized with ZnO nanotubes [17] or nanorods [1]. It can be specially noted that the TiO_2/CdS and ZnO/CdS quantum dots sensitized solar cells (QDSSC) with conversion efficiencies of over 1 % were reported in the recent past. CdS is also used as the acceptor in many PV devices with conjugated polymers such as MEH: PPV [18, 19] and P3HT [20, 21].

P3HT sensitized porous CdS based solar cells with PEDOT:PSS/Au top contact showed a conversion efficiency of around 0.3 %, and improved up to 1.2 % with N719 dye as the interface modifier [22]. Additionally, well aligned CdS nanorods with MEH:PPV showed maximum efficiency of 0.6 % [19]. PCE of 0.87 % was reported for TiO_2 nanocrystalline solar cells with CdS, 2-amino-1-methyl-benzimidazole, and P3HT with silver top contact [23].

In this work, we deposited CdS nanolayer on nanoporous TiO_2 using chemical bath deposition (CBD) technique to study the use of CdS layer as an interface modifier and co-sensitizer on improving the performance of hybrid TiO_2–P3HT PV devices.

2 Experimental procedure

Samples were prepared on indium tin oxide coated glass substrates (ITO, 12 × 12 mm, 10–15 Ω/square), which were first cleaned by ultrasonic agitation in acetone and 2-propanol. Cleaned substrates were then covered with a dense layer of TiO_2 (thickness $\sim$50 nm) by spray pyrolysis. Porous layer of TiO_2 nanocrystalline film of thickness about 600 nm was deposited onto the dense layer by spin coating commercially available TiO_2 paste (DSL 18NRT, Dyesol) diluted with tetrahydrofuran (THF) followed by sintering at 450 °C for an hour.

The CdS layer was deposited by chemical bath deposition (CBD) using aqueous solutions of cadmium chloride ($CdCl_2$), thiourea ($(NH_2)_2CN$), ammonium chloride (NH_4Cl) and ammonium hydroxide (NH_4OH). 0.033 M of cadmium chloride and 0.066 M of thiourea were used as cadmium and sulfur ion sources, respectively. 1 M of ammonium chloride and NH_4OH were used as buffer solution and complex agent, respectively to control the reaction rate. The reaction bath contained 250 ml of de-ionized and de-gassed water heated at 80 °C and stirred at a constant rate of 240 rpm with the help of a magnetic stirrer. The substrates were kept vertically so that the TiO_2 deposited surface facing the center of the reaction bath. The prepared solutions; 8 ml of NH_4OH, 4 ml of cadmium chloride, and 2 ml ammonium chloride were added in an interval of 1 min and the temperature of the bath was raised up to 85 °C. Thereafter, the thiourea solution was titrated by 1 ml doses for four times in an interval of 1 min. The system was kept at a constant temperature of 85 °C for 8 min and continuously stirred.

The CdS deposited samples were then removed from the bath and rinsed by de-ionized water followed by a sintering at 320 °C for 20 min to ensure the removal of chemical residues and water. The samples were then dipped into 1 mg/ml of P3HT polymer (Merck Chemicals Limited, Darmstadt, Germany) solution for 12 h. Another layer of P3HT was deposited by spin coating with precursor concentration of 25 mg/ml at 1250 rpm for 30 s. Again the samples were dried and annealed at 110 °C in nitrogen environment. The top contact was made by thermal evaporation of gold after deposition of a poly (ethylene dioxythiophene): polystyrene sulfonate (PEDOT:PSS) layer, as reported by Ravirajan et al. [24]. Six devices were fabricated in a single substrate and the control devices with TiO_2 and P3HT were made without CdS deposition. All other fabrication methods were carried out in the same condition for both control and CdS deposited devices.

UV–Vis spectrometer (JENWAY) was used to measure the optical absorption spectra of active layer prior to metal deposition. The surface morphology of the spin coated TiO_2 and CdS deposited on TiO_2 layers were analyzed by field-emission scanning electron microscope (FESEM, Auriga, Zeiss Ultra-60). Photovoltaic performance of the devices was studied by measuring photocurrent spectra and current density and voltage (J–V) characteristics under light illumination. For electrical characterization, the devices were housed in a home built sample holder with a glass window. The sample holder was evaluable to a pressure of $<10^{-1}$ mbar and all the measurement were taken under vacuum. External quantum efficiency (EQE) spectra were calculated from short circuit photocurrent spectra by comparison of the photo response with that of a calibrated silicon photodiode (Newport). Current–voltage (I–V) characteristics in the dark were measured before and after the illuminated I–V characteristic in order to confirm that the device behavior had not changed. I–V characteristics were also measured under simulated sunlight using

Keithley 2600 source measure unit and a solar simulator (SCIENCETECH) with AM 1.5 filter. For PV transient measurements, a digital storage oscilloscope (Tektronix, TDS1012B) and a pulsed laser (Big Sky Laser, Ultra-having illumination cycle—6nS, power—10 mJ and wavelength—532 nm) were used.

3 Results and discussion

Figure 1 compares FESEM images of nanoporous TiO_2 film and CdS coated TiO_2 film after thermal annihilation. These images confirm that CdS is uniformly coated on the surface of nanocrystalline TiO_2 films and is reduced the pore size of the TiO_2 film.

Figure 2 shows optical absorption spectra of CdS, P3HT, CdS/P3HT coated TiO_2 films and bare TiO_2 film. CdS film was coated by chemical bath deposition while P3HT on TiO_2 or TiO_2/CdS films were coated by dipping the respective electrodes in P3HT/chlorobenzene solution. CdS layer broadens absorption of active layers (350–650 nm) with an additional absorption peak at 450 nm (see Fig. 2). This observation is consistent with reports in the literature [25]. Combined TiO_2/CdS/P3HT thin films show wide response to the visible spectra and its absorption is reduced with the addition of CdS due to lower polymer uptake as the pores of the films were filled with CdS (Fig. 1b). This may also be due to the reduced reflectance of CdS coated TiO_2 film [26].

Figures 3a, b show that a significant improvement was observed in the performance of TiO_2/CdS/P3HT cell in comparison with similar device without having CdS layer. Short circuit current (J_{SC}) of 5.91 mA/cm^2 and an open circuit voltage (V_{OC}) of 0.57 V with a fill factor of 36 % were observed for TiO_2/CdS/P3HT cells, which showed the

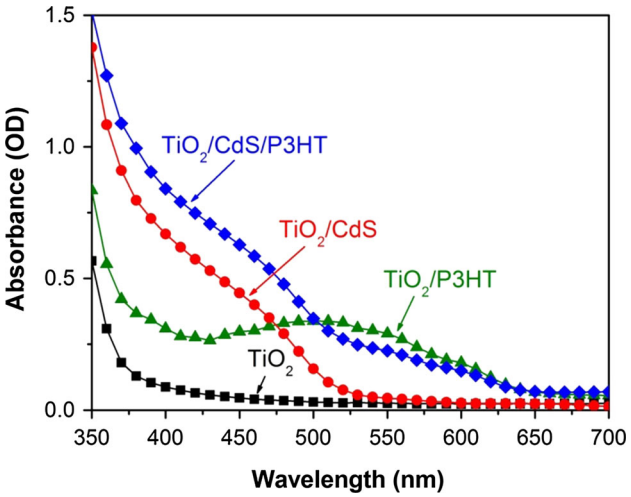

Fig. 2 Absorption spectra of TiO_2, TiO_2/CdS, TiO_2/P3HT and TiO_2/CdS/P3HT films

overall average power conversion efficiency over 1.5 % with a champion cell efficiency of over 2.2 %. However, the device without CdS showed nearly 0.5 % of conversion efficiency with J_{SC} of 3.5 mAcm^{-2} and V_{OC} of 0.35 V with a fill factor of 27 %. The three fold increase in the PCE of TiO_2/CdS/P3HT cell could be ascribed to the significant improvement in the J_{SC}, V_{OC} and fill factor.

The improved fill factor can be attributed to the avoided device shunting and closely filled cell stack. The improvement in V_{OC} could be due to the presence of CdS layer in the cell structure and its involvement in free carrier generation [27, 28]. As reported by Brabec et al. [29], the V_{OC} of polymer based solar cells are limited by the difference between the HOMO of the donor and the LUMO of the acceptor. In TiO_2/polymer hybrid solar cells, it has been shown that V_{OC} is limited by the difference between

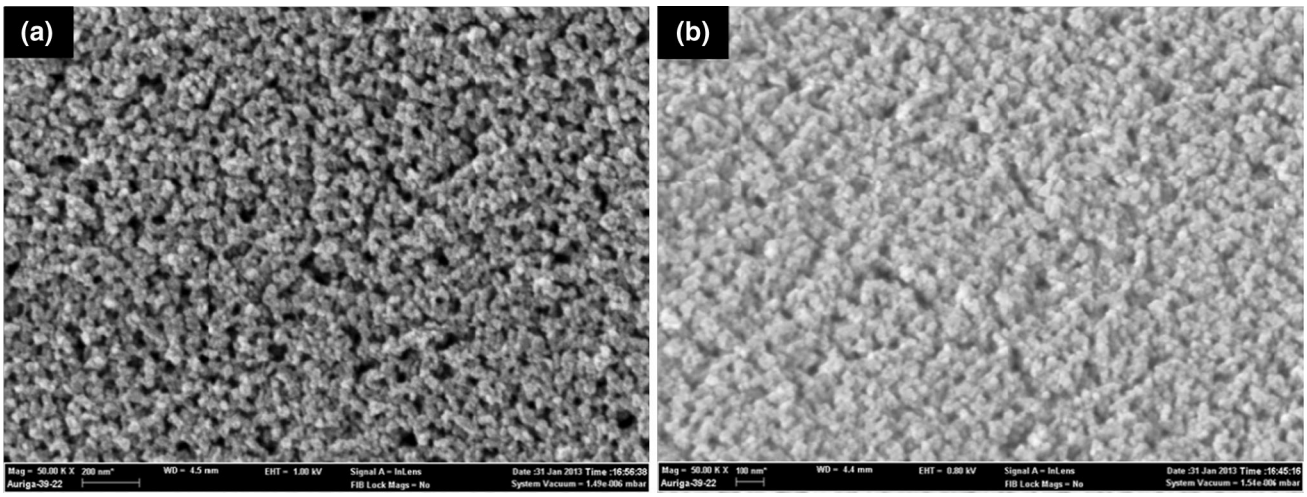

Fig. 1 FESEM images of **a** spin coated porous TiO_2, and **b** CdS coated TiO_2 films after thermal annihilation at 320 °C

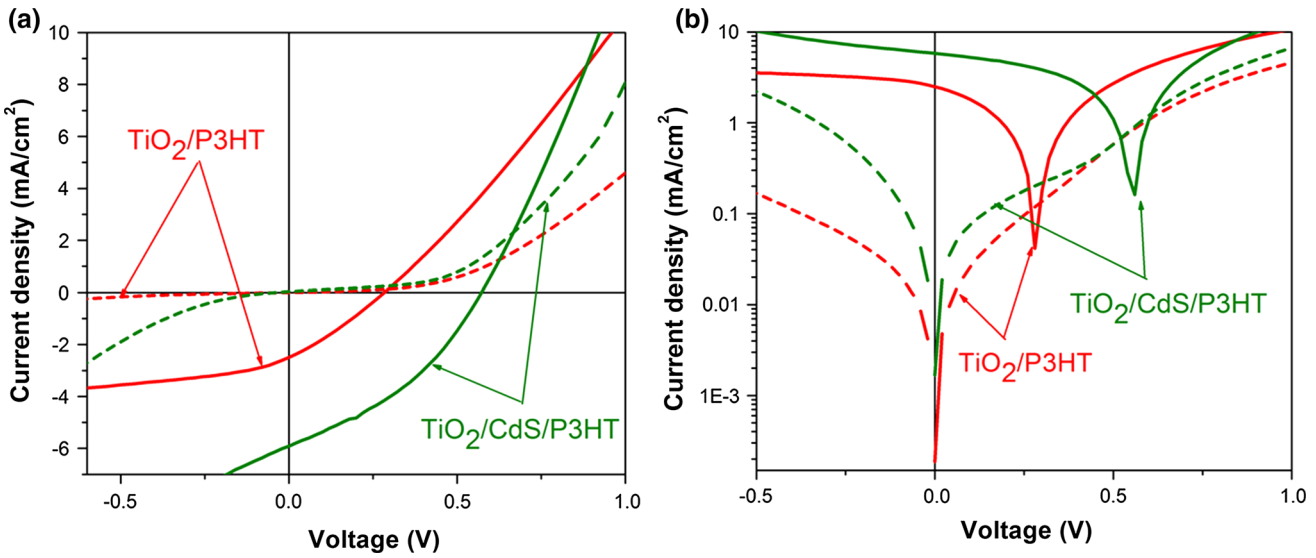

Fig. 3 **a** The current density–voltage (J–V) characteristic curves of the ITO/TiO_2/P3HT/PEDOT:PSS/Au and ITO/TiO_2/CdS/P3HT/PEDOT:PSS/Au solar cells under dark (*dashed lines*) and under illumination of intensity 70 mW/cm^2 (*solid lines*) with A.M 1.5 filter, and **b** the same graphs replotted in semi-log scale with clear evidence of improved V_{OC} and reduced short circuited dark current density

HOMO of the polymer and the conduction band (CB) edge of TiO_2 [30].

Figures 4a, b illustrate the proposed electronic energy level diagram of ITO/TiO_2/P3HT/PEDOT/Au and ITO/TiO_2/CdS/P3HT/PEDOT:PSS/Au, respectively. It shows that the energy separation between the HOMO of P3HT and CB edge of TiO_2 is nearly 0.7 eV. With the addition of CdS interlayer, which may acts as both donor and acceptor in the cell, the separation between the donor's HOMO and acceptor's CB edge of acceptor is increased from 0.7 to 1.0 eV, which is consistent with the improved V_{OC} found in TiO_2/CdS/P3HT devices. The improved V_{OC} can also be explained by the involvement of CdS in carrier generation [31].

Figure 5 shows the external quantum efficiency spectra of TiO_2/P3HT and TiO_2/CdS/P3HT solar cells and their corresponding absorbance spectra of the corresponding active layer without top contact. External quantum efficiency spectra of TiO_2/CdS/P3HT resemble the absorbance feature of CdS and P3HT as well as of TiO_2. Insertion of CdS layer at the nanocrystalline TiO_2/P3HT interface, broadens quantum efficiency spectrum of the solar cells with peak values over 80 and 40 % at the maximum absorption of CdS and P3HT, respectively. This further

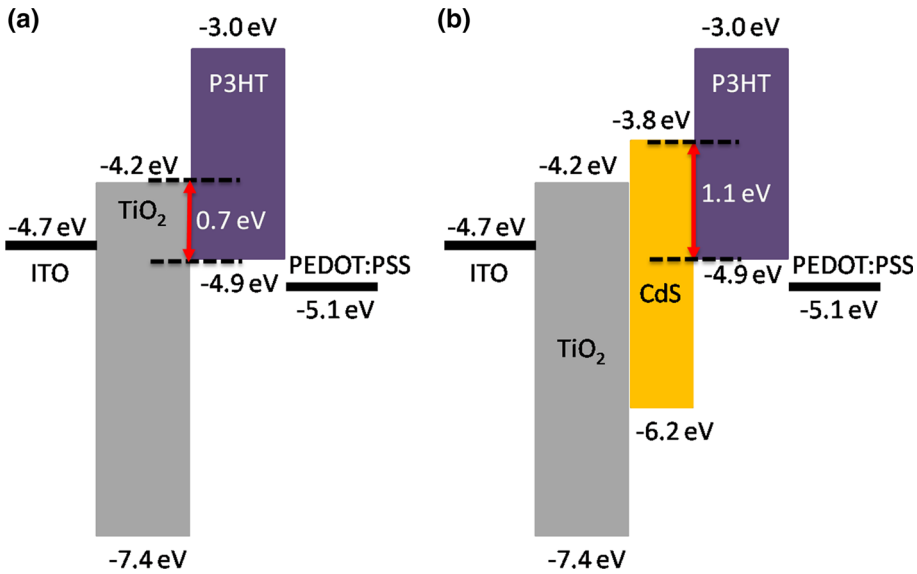

Fig. 4 Proposed electronic energy level diagram of **a** TiO_2/P3HT, and **b** TiO_2/CdS/P3HT solar cells with ITO and PEDOT:PSS/Au as bottom and top electrodes, respectively

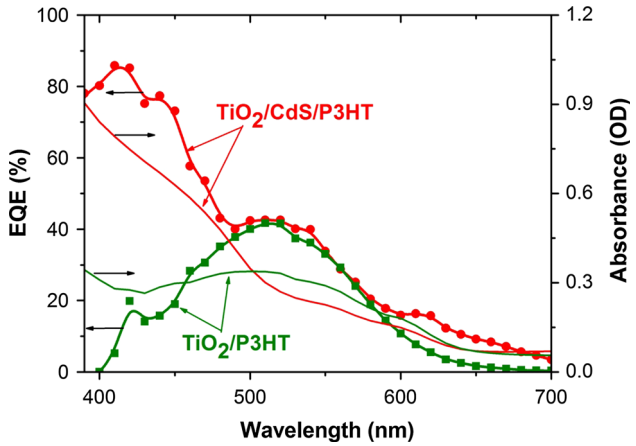

Fig. 5 External quantum efficiency spectra of ITO/TiO_2/P3HT/PEDOT/Au (*Square*) and ITO/TiO_2/CdS/P3HT/PEDOT:PSS/Au (*circle*) solar cells and absorbance spectra of the corresponding TiO_2/P3HT and TiO_2/CdS/P3HT thin films

confirms the involvement of CdS in the process of free carrier generation and the safe passage of charge carriers to the electrodes assisted by P3HT layer. The presence of CdS also improves the transport of electrons from the polymer to TiO_2, and holes from TiO_2 to P3HT by providing an intermediate level [32].

Photovoltaic transient measurement is one of the efficient methods to study the charge carrier recombination kinetics in thin film PV devices. Figure 6 shows the PV transient measurements of TiO_2/P3HT and TiO_2/CdS/P3HT cells. An excitation laser with 532 nm wavelength was used to selectively excite the polymer and study the effect of CdS inter-layer on the life time of charge carriers induced in polymer layer. As there is no optical absorption by the CdS at 532 nm, it can be assumed that the CdS layer would not contribute any free carriers during the illumination and the total energy from the laser pulse will be transferred to the

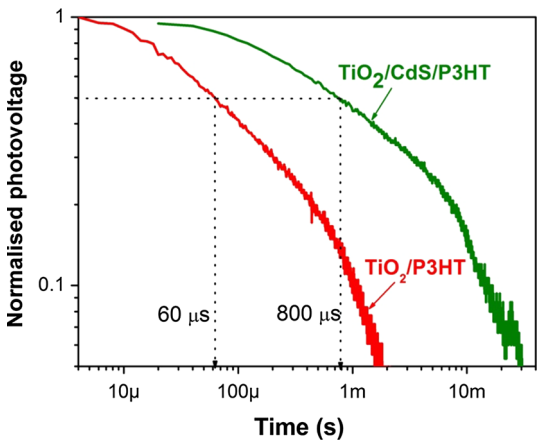

Fig. 6 Double logarithmic normalized photovoltaic transient decay patterns of ITO/TiO_2/P3HT/PEDOT/Au and ITO/TiO_2/CdS/P3HT/PEDOT:PSS/Au cells

P3HT film. The carrier life time in the CdS modified devices was found to be 800 µs, which is more than an order of magnitude greater than that in TiO_2/P3HT devices. This study reveals that the recombination of carriers generated in polymer layer is slower in the devices with CdS interface layer. The CdS also prevents the recombination of free carriers and ensures better charge collection at the electrodes. Similar observation was reported by Loheeswaran et al. [33] using an insulating alumina monolayer at the TiO_2/P3HT interface.

4 Conclusions

In conclusion, we find that insertion of cadmium sulfide (CdS) layer at the nanocrystalline TiO_2/P3HT interface broadens quantum efficiency spectrum of the solar cells and controls recombination kinetics. TiO_2/P3HT solar cells with CdS interlayer yield PCEs over 1.5 %, which is three times greater than that for similar solar cells without CdS layer. A cascade structure with proper channels is more effective to improve the performance of P3HT based hybrid PV devices. The possible applications of CdS as the interface modifier and co-sensitizer in organic solar cells are verified and the results show the multifunction of P3HT as the photon absorber and hole conductor in solid state hybrid PV devices.

Acknowledgments Authors acknowledge Dr. K. Vignarooban for his critical discussion during preparation of this manuscript. P. R and K. B acknowledge the National Research Council (NRC), Sri Lanka and Sivananthan Laboratories Inc. USA for financial assistance (Research Grant No. 11-175) and their training at the laboratory, respectively.

References

1. A.M. Peiro, P. Ravirajan, K. Govender, D.S. Boyle, P. O'Brien, D.D.C. Bradley, J. Nelson, J.R. Durrant, J. Mater. Chem. **16**, 2088 (2006)
2. H.J. Snaith, C. Ducati, Nano Lett. **10**, 1259 (2010)
3. P. Ravirajan, S.A. Haque, D. Poplavskyy, J.R. Durrant, D.D.C. Bradley, J. Nelson, Optical Science and Technology, SPIE's 48th Annual Meeting, International Society for Optics and Photonics, pp 226–236 (2004)
4. P. Ravirajan, A.M. Peiro, M.K. Nazeeruddin, M. Graetzel, D.D.C. Bradley, J.R. Durrant, J. Nelson, J. Phys. Chem. B **110**, 7635 (2006)
5. G.K. Mor, S. Kim, M. Paulose, O.K. Varghese, K. Shankar, J. Basham, C.A. Grimes, Nano Lett. **9**, 4250 (2009)
6. R. Zhu, C.Y. Jiang, B. Liu, S. Ramakrishna, Adv. Mater. **21**, 994 (2009)
7. J. Boucle, P. Ravirajan, J. Nelson, J. Mater. Chem. **17**, 3141 (2007)
8. P. Ravirajan, S.A. Haque, J.R. Durrant, D. Poplavskyy, D.D.C. Bradley, J. Nelson, J. Appl. Phys. **95**, 1473 (2004)
9. L. Dou, J. You, J. Yang, C.C. Chen, Y. He, S. Murase, T. Moriarty, K. Emery, G. Li, Y. Yang, Nat. Photonics **6**, 180 (2012)

10. V. Shrotriya, E.H.E. Wu, G. Li, Y. Yao, Y. Yang, Appl. Phys. Lett. **88**, 064104 (2006)
11. F. Wu, Q. Cui, Z. Qiu, C. Liu, H. Zhang, W. Shen, M. Wang, ACS Appl. Mater. Interfaces **5**, 3246 (2013)
12. A. Braga, S. Gimenez, I. Concina, A. Vomiero, I.M. Mora-Sero, J. Phys. Chem. Lett. **2**, 454 (2011)
13. V.G. Pedro, C. Sima, G. Marzari, P.P. Boix, S. Gimenez, Q. Shen, T. Dittrich, I. Mora-Sero, Phys. Chem. Chem. Phys. **15**, 13835 (2013)
14. C. Li, L. Yang, J. Xiao, Y.C. Wu, M. Sondergaard, Y. Luo, D. Li, Q. Meng, B.B. Iversen, Phys. Chem. Chem. Phys. **15**, 8710 (2013)
15. J. Kim, H. Choi, C. Nahm, C. Kim, J. Ik Kim, W. Lee, S. Kang, B. Lee, T. Hwang, H. Hejin Park, B. Park, Appl. Phys. Lett. **102**, 183901 (2013)
16. H.J. Lee, J. Bang, J. Park, S. Kim, S.M. Park, Chem. Mater. **22**, 5636 (2010)
17. S. Banerjee, S.K. Mohapatra, P.P. Das, M.S. Misra, Chem. Mater. **20**, 6784 (2008)
18. L. Wang, Y. Liu, X. Jiang, D. Qin, Y. Cao, J. Phys. Chem. C **111**, 9538 (2007)
19. Y. Kang, D. Kim, Sol. Energy Mater. Sol. Cells **90**, 166 (2006)
20. X. Jiang, F. Chen, Q. Weiming, Q. Yan, Y. Nan, H. Xu, L. Yang, H. Chen, Sol. Energy Mater. Sol. Cells **94**, 2223 (2010)
21. H.C. Leventis, S.P. King, A. Sudlow, M.S. Hill, K.C. Molloy, S.A. Haque, Nano Lett. **10**, 1253 (2010)
22. M. Zhong, D. Yang, J. Zhang, J. Shi, X. Wang, C. Li, Sol. Energy Mater. Sol. Cells **96**, 160 (2012)
23. N. Balis, V. Dracopoulos, E. Stathatos, N. Boukos, P. Lianos, J. Phys. Chems. C **115**, 10911 (2011)
24. P. Ravirajan, D.D.C. Bradley, J. Nelson, S.A. Haque, J.R. Durrant, H.J.P. Smit, J.M. Kroon, Appl. Phys. Lett. **86**, 143101 (2005)
25. C. Goh, S.R. Scully, M.D. McGehee, J. Appl. Phys. **101**, 114503 (2007)
26. X.F. Gao, W.T. Sun, Z.D. Hu, G. Ai, Y.L. Zhang, S. Feng, F. Li, L.M. Peng, J. Phys. Chem. C **113**, 20481 (2009)
27. E.D. Spoerke, M.T. Lloyd, E.M. McCready, D.C. Olson, Y.J. Lee, J.W.P. Hsu, Appl. Phys. Lett. **95**, 213506 (2009)
28. L.X. Reynolds, H. Lutz, S. Dowland, A. MacLachlan, S. King, S.A. Haque, Nanoscale **4**, 1561 (2012)
29. C.J. Brabec, A. Cravino, D. Meissner, N.S. Sariciftci, T. Fromherz, M.T. Rispens, L. Sanchez, J.C. Hummelen, Adv. Funct. Mater. **11**, 374 (2001)
30. T. Ishwara, D.D.C. Bradley, J. Nelson, P. Ravirajan, I. Vanseveren, T. Cleij, D. Vanderzande, L. Lutsen, S. Tierney, M. Heeney, I. McCulloch, Appl. Phys. Lett. **92**, 053308 (2008)
31. J. Hou, M.H. Park, S. Zhang, Y. Yao, L.M. Chen, J.H. Li, Y. Yang, Macromolecules **41**, 6012 (2008)
32. M.C. Scharber, D. Mühlbacher, M. Koppe, P. Denk, C. Waldauf, A.J. Heeger, C.J. Brabec, Adv. Mater. **18**, 789 (2006)
33. S. Loheeswaran, K. Balashangar, J. Jevirshan, P. Ravirajan, J. Nanoelectron. Optoelectron **8**, 484 (2013)